Formation of Molecular Templates Containing Cumulative Double Bonds (C=C=C) at Organic/Silicon Hybrid Interfaces

Hai Gou Huang, Jing Yan Huang, Yong Ping Zhang, Yue Sheng Ning, Kian Soon Yong, and Guo Qin Xu*

Department of Chemistry, National University of Singapore, 10 Kent Ridge, Singapore, 119260

Received: August 13, 2004; In Final Form: November 19, 2004

The cumulative double bond (C=C=C), an important intermediate in synthetic organic chemistry, was successfully prepared via the selective attachment of acetylethyne to Si(111)-7 × 7. The experimental observation of the characteristic vibrational modes and electronic structures of the C=C=C group in the surface species demonstrates the [4 + 2]-like cycloaddition occurring between the terminal O and C atoms of acetylethyne and the neighboring Si adatom−rest atom pair, consistent with the prediction of density functional theory calculations. Scanning tunneling microscopy images further reveal that the molecules selectively bind to the adjacent adatom−rest atom pairs on Si(111)-7 × 7.

I. Introduction

The intense interest in studying reactions of organic molecules on semiconductor surfaces mainly arises from its potential applications in the development of sensors, molecular electronics, and nanotechnology.[1−3] To create organic-functionalized semiconductor surface structures with custom-tailored properties, attaching multifunctional organic molecules onto the surface in a controllable and selective manner is essentially required. To achieve this goal, it is very important to gain a detailed understanding of the selectivity, configuration, and mechanisms of multifunctional organic molecules binding on silicon surfaces.

The Si(111)-7 × 7 surface adopts the dimer-adatom-stacking (DAS) fault structure (Figure 1a).[4,5] This surface provides a number of chemically, spatially, and electronically inequivalent reactive sites, including the adatoms and rest atoms in the inherently different faulted and unfaulted halves and corner holes. Adjacent adatom−rest atom pairs on Si(111)-7 × 7 were found to be diradical-like (Figure 1b) and to undergo [2 + 2]-like cycloaddition with simple alkenes (e.g., ethylene)[6,7] and alkynes (e.g., acetylene)[8−10] as well as a [4 + 2]-like reaction ("4" refers to the number of participating adsorbate atoms inside the resulting adduct ring upon adsorption, and "2" simply refers to the two participating surface atoms, which may or may not be adjacent to each other) with conjugated organic molecules.[11−14]

In this paper, the covalent attachment chemistry of acetylethyne (CH≡C−C(CH_3)=O) on Si(111)-7 × 7 was studied with the objectives of elucidating the acetylethyne/Si(111)-7 × 7 interfacial reaction mechanism and developing a functional intermediate suitable for further organic syntheses and functionalization. High-resolution electron energy loss spectroscopy (HREELS) was used to characterize the vibrational properties of acetylethyne on Si(111)-7 × 7. X-ray photoelectron spectroscopy (XPS) provided information on chemical shifts of the C 1s and O 1s core levels. Scanning tunneling microscopy (STM) was employed to investigate the spatial distribution and selectivity of this surface reaction system at atomic resolution. Density functional theory (DFT) calculations (pBP/DN** in Spartan 5.1) were commanded to optimize the chemisorption geometries and calculate their adsorption energies and vibrational frequencies. Our experimental results, together with DFT calculations, show that acetylethyne is covalently bonded to Si(111)-7 × 7 mainly through a [4 + 2]-like cycloaddition of the C≡C−C=O skeleton with the adjacent adatom−rest atom pair. The formed cumulative double bonds C=C=C may be considered as a precursor for realizing "dry" organic syntheses on the Si(111) surface and further functionalization.

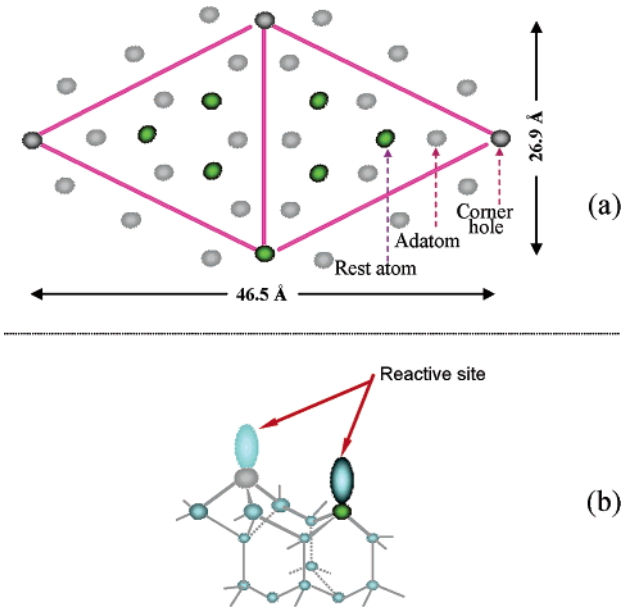

Figure 1. (a) Top view of Si(111)-7 × 7 structure on the basis of dimer-adatom-stacking (DAS) fault; (b) reactive sites of an adjacent adatom−rest atom pair.

II. Experimental Section

The experiments were performed in three separate ultrahigh vacuum (UHV) chambers. All of them have a base pressure of $<2 \times 10^{-10}$ Torr, achieved with turbomolecular and sputter-ion pumps. The first UHV chamber is equipped with an X-ray

* Corresponding author. Fax: (65) 6779 1691. E-mail: chemxugq@nus.edu.sg.

10.1021/jp046347w CCC: $30.25
Published on Web 02/24/2005

gun (both Mg and Al anodes), He-discharge UV source, and hemispherical energy analyzer (CLAM 2, VG) for X-ray photoelectron spectroscopy (XPS) and ultraviolet photoelectron spectroscopy (UPS), respectively. The HREELS chamber mainly consists of a high-resolution electron energy loss spectrometer (HREELS, LK-2000-14R) and a quadrupole mass spectrometer (UTI-100) for gas analysis. The scanning tunneling microscopy (STM) system includes a sample preparation system and Omicron VT STM chamber.

For HREELS experiments, the electron beam with an energy of 5.0 eV impinges on Si(111)-7 × 7 at an incident angle of 60° with a resolution of 6−7 meV (fwhm, 50 cm^{-1}). XPS spectra were acquired using Mg Kα radiation ($h\nu$ = 1253.6 eV) and a 20 eV pass energy. For XPS, the binding energy (BE) scale is referenced to the peak maximum of the Si 2p line (99.3 eV calibrated for Au $4f_{7/2}$)[15] of a clean Si (111)-7 × 7 substrate. The spectra of the physisorbed multilayer and saturated chemisorption monolayer were fitted with the software VGX900 (VG Scientific, UK). During the fitting, the full width at half-maximum (fwhm) of each peak was kept at 1.2 eV, which is the typical resolution of the C 1s core level for our XPS system. The constant current topographs (CCTs) of the clean and acetylethyne-exposed Si(111)-7 × 7 were usually obtained with a sample bias of V_s = 1−2 V and a tunneling current of I_t = 0.15−0.2 nA.

For HREELS and XPS experiments, the samples with dimensions of 8 × 18 × 0.35 mm^3 (2 × 12 × 0.5 mm^3 for STM experiment) were cut from n-type Si (111) wafers (phosphorus-doped, with a resistivity of 1−30 Ω·cm, 99.999%, Goodfellow); a Ta-sheet heater (0.025 mm thick, Goodfellow) is sandwiched tightly between two Si(111) crystals held together by two Ta clips. Uniform heating of the samples is achieved by passing current through the Ta heater. This sample mounting configuration allows us to resistively heat the samples to 1400 K and conductively cool them to 110 K using liquid nitrogen. Sample mounting for STM is different. The Si(111) wafer is directly mounted to the sample holder and can be flashed to 1200 °C. The temperature distribution on the samples is within ±10 K at 1000 K, determined using a pyrometer (ϵ = 0.74, TR-630, Minolta).

The Si(111) sample was cleaned by repeated ion sputtering−annealing cycles (500 eV Ar^+ bombardment for 30 min with an ion current density of ∼5 μA·cm^{-1} and subsequent annealing to 1250 K for 20 min). The surface cleanliness was routinely monitored using STM, XPS, and HREELS. The 7 × 7 reconstruction was formed after the final annealing procedure. Acetylethyne (Aldrich, 95.0%) was purified by freeze−pump−thaw cycles and dosed onto Si(111)-7 × 7 through a variable leaking valve without the calibration of ion gauge sensitivity.

III. Results

III.A. High-Resolution Electron Energy Loss Spectroscopy. Figure 2 shows the high-resolution electron energy loss spectra of the physisorbed acetylethyne ($C^1H{\equiv}C^{2-}C^3(C^4H_3){=}O$) and the saturated chemisorption monolayer on Si(111)-7 × 7. The vibrational frequencies and their assignments for physisorbed and chemisorbed acetylethyne are listed in Table 1. A condensed multilayer acetylethyne is formed after exposing 8.0 L onto the Si(111)-7 × 7 at 110 K. For this surface (Figure 2a), the energy-loss peaks at 580, 708, 979, 1195, 1412, 1684, 2100, 2931, and 3240 cm^{-1} are readily resolved, which are in good agreement with the IR and Raman spectroscopic data of liquid-phase acetylethyne within ∼15 cm^{-1}.[16] Among these vibrational signatures, the two peaks at 3240 and 2931 cm^{-1} are assigned to the C−H stretching modes of the ≡CH and $-CH_3$ groups, respectively. The features at 1684 and 2100 cm^{-1} are related to the C═O and C≡C stretching modes, respectively.

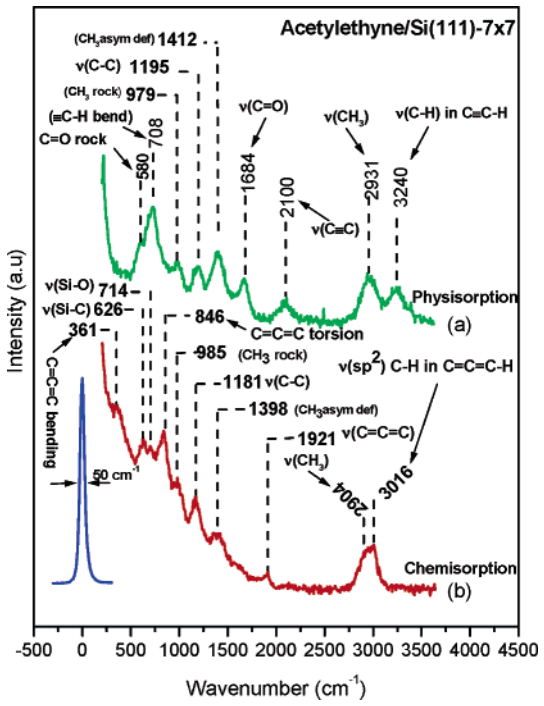

Figure 2. HREELS spectra of physisorbed and saturated chemisorption acetylethyne on Si(111)-7 × 7.

The vibrational features of chemisorbed acetylethyne were obtained by annealing the multilayer acetylethyne-covered sample to 300 K to drive away all physisorbed molecules and retain only the chemisorbed monolayer (Figure 2b). Losses at 361, 626, 714, 846, 985, 1181, 1398, 1921, 2904, and 3016 cm^{-1} can be identified. The absence of the Si−H stretching around 2050 cm^{-1} [17] suggests the nature of molecular chemisorption for acetylethyne on Si(111)-7 × 7. The disappearance of C═O (at 1684 cm^{-1}) and C≡C (at 2100 cm^{-1}) stretching modes in the chemisorbed molecules strongly demonstrates their simultaneous involvement in the surface binding, clearly ruling out the possibility of the [2 + 2]-like cycloaddition occurring only through the C═O group or the C≡C group. The major spectroscopic change is the appearance of a new peak at 1921 cm^{-1}, ascribed to the characteristic vibration of a C═C═C skeleton (asymmetric stretching mode).[18−20] This assignment is further supported by the concurrent observation of its torsion (846 cm^{-1}) and bending (361 cm^{-1}) modes. Furthermore, the two new peaks at 626 and 714 cm^{-1} are ascribed to the Si−C and Si−O stretching modes,[11,21] respectively. An additional new feature is noticed at 3016 cm^{-1}, assigned to the (sp^2) C−H stretching vibration. This result shows the rehybridization of C^1 atom of the $C^2{\equiv}C^1H$ group from sp to sp^2 due to its binding with the Si dangling bond. Our main vibrational results of chemisorbed acetylethyne strongly suggest the formation of an allenic-like surface intermediate containing a $-CH{=}C{=}C(CH_3)-O-$ skeleton through the reaction of both $\pi_{C=O}$ and $\pi_{C\equiv C}$ bonds with an adjacent adatom−rest atom pair via the [4 + 2]-like process. Table 1 also lists the main vibrational frequencies of the $Si-CH{=}C{=}C(CH_3)-O-Si$ structure from our DFT calculations, further confirming our assignments for chemisorbed acetylethyne on Si(111)-7 × 7. The details of DFT theoretical modeling will be given in section III.D.

III.B. X-ray Photoelectron Spectroscopy. Figure 3 presents the O 1s XPS spectra for physisorbed and chemisorbed

TABLE 1: Assignment of Vibrational Modes for Physisorbed and Chemisorbed Acetylethyne on Si(111)-7 × 7[a]

vibr assignt	IR liquid[16]	Raman liquid[16]	physisorbed[b]	vibr assignt	chemisorbed[b]	calcd[b]
≡CH stretching	3359, 3262		3240	−CH= stretching	3016	3025
$-CH_3$ stretching	3011(a), 2972(a), 2921(s)	3017(a), 2978(a), 2926(s)	2931	$-CH_3$ stretching	2904	2940(a), 2894(s)
C≡C stretching	2099	2092	2100	C=C=C asymmetric stretch	1921	1935
C=O stretching	1690	1685	1684	$-CH_3$ deformation	1398	1412(a),136 4 (s)
$-CH_3$ deformation	1426(a), 1364(s)	1429(a), 1368(s)	1412	C−C stretching	1181	1139
C−C stretching	1198	1198	1195	CH_3 rock	985	1020, 967
CH_3 rock	1022, 981	1027, 983	979	C=C=C torsion	846	830
≡C−C stretching	741	743		Si−O stretching	714	701
≡CH bending	700	700	708	Si−C stretching	626	624
C=O rock	587	590	580	C=C=C bending	361	371
CH_3 torsion	435	436				
C−C≡C bending	228	230, 183				

[a] IR and Raman data[16] for liquid acetylethyne are included for comparison (the vibrational frequencies are given in cm^{-1}). [b] Present work.

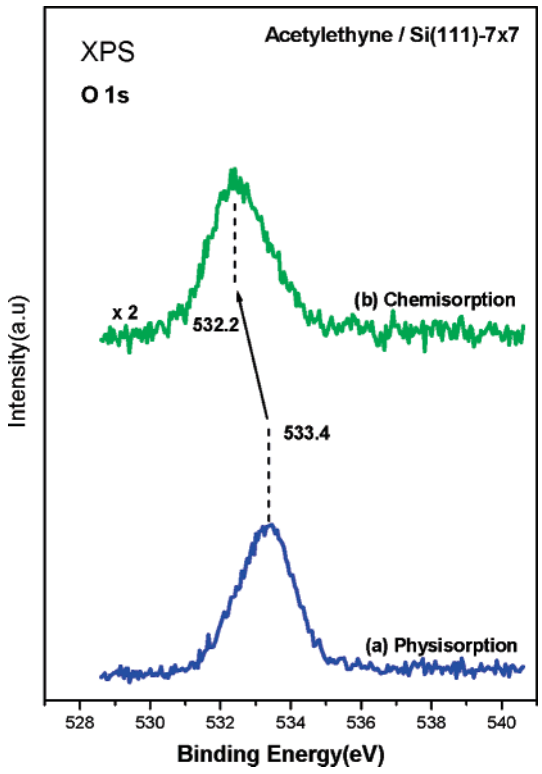

Figure 3. O 1s XPS for physisorbed and chemisorbed acetylethyne on Si(111)-7 × 7.

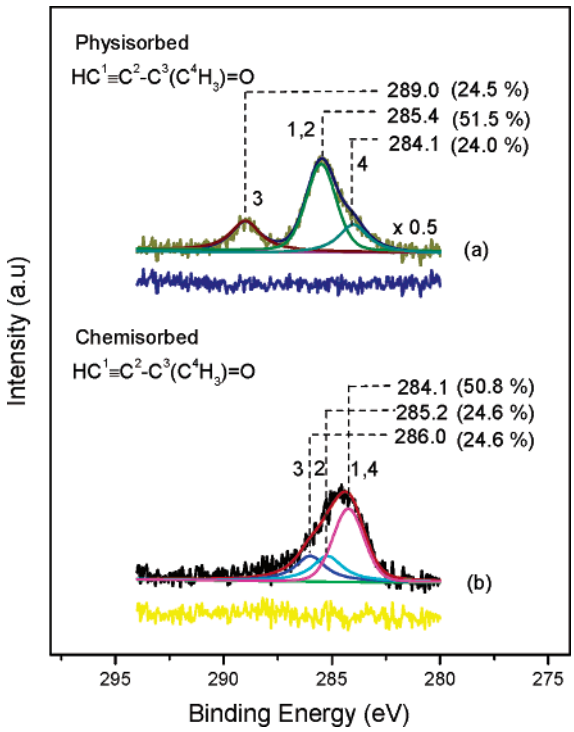

Figure 4. Fitted C 1s spectra for physisorbed and saturated chemisorbed acetylethyne on Si(111)-7 × 7.

acetylethyne on Si(111)-7 × 7. The O 1s photoemission spectrum of physisorbed molecules (Figure 3a) shows a symmetric peak at 533.4 eV with a typical fwhm (∼1.2 eV) under our XPS resolution. The 533.4 eV binding energy observed here is close to the value observed for oxygen atoms in molecules containing intact carbonyl groups.[21−23] Compared to the physisorption spectrum, the O 1s (532.2 eV) core level of chemisorbed molecules (Figure 3b) displays a downshift of 1.2 eV, implying the direct involvement of the O atom in acetylethyne binding on Si(111)-7 × 7. This value is in good agreement with results obtained for other molecules covalently attached to the surface through the Si−O bond.[22,23]

Figure 4 shows the fitted C 1s XPS spectra for physisorbed and chemisorbed $C^1H{\equiv}C^{2-}C^3(C^4H_3){=}O$ on Si(111)-7 × 7. The C 1s spectrum of physisorbed molecules is deconvoluted into three peaks centered at 289.0, 285.4, and 284.1 eV with an area ratio of 1:2:1 (Figure 4a). The peak at 289.0 eV can be assigned to the C atom of carbonyl, similar to the value obtained in molecules containing intact carbonyl groups on Si(111) surface.[21,22] The photoemission features at 285.4 and 284.1 eV are associated with $C^1H{\equiv}C^{2-}$ and $-C^4H_3$, respectively, in good agreement with the C 1s BEs determined for the C atoms with sp and sp^3 hydridizations.[24,25]

For chemisorbed acetylethyne (Figure 4b), the C 1s spectrum is significantly different, which implies large changes in electronic structures upon chemisorption. It can be fitted into three peaks at 286.0, 285.2, and 284.1 eV with an area ratio of 1:1:2. A detailed discussion of this difference and the assignments of the three peaks in Figure 4b will be presented in section IV.

III.C. Scanning Tunneling Microscopy. To further elucidate site selectivity of acetylethyne binding on Si(111)-7 × 7, STM was used to investigate the extent and spatial distribution of the present surface reaction system at atomic resolution. Figure 5a shows STM constant current topograghs (CCTs) of a clean Si(111)-7 × 7surface at room temperature with a defect density of <0.5%, estimated by counting an area containing about 1500 adatoms. Figure 5b is the typical STM topograph of Si(111)-7 × 7 exposed to 0.4 L (direct dosing) of acetylethyne at room temperature. Comparison with the clean and acetylethyne-covered surfaces reveals that the 7 × 7 reconstruction is

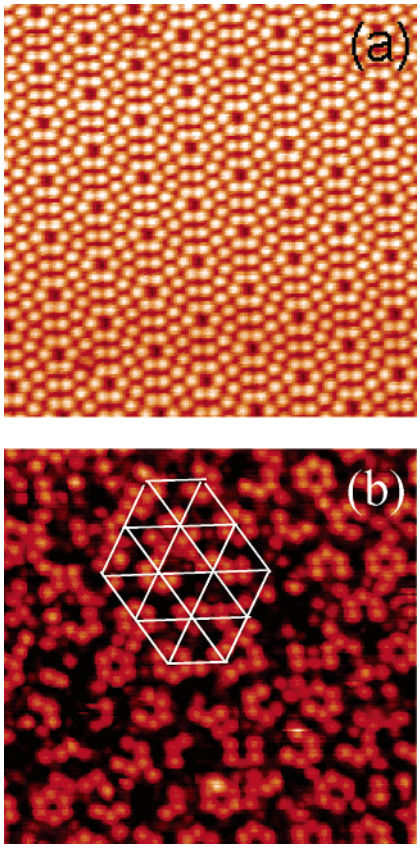

Figure 5. Constant current topograph (CCT) images (~200 Å × 200 Å, $V_s = +1.0$ V, $I_t = 0.15$ nA) of clean (a) and saturated chemisorption acetylethyne (b) on Si(111)-7 × 7 at 300 K.

preserved after the acetylethyne adsorption reaction. However, some adatoms become invisible as a result of reaction, increasing in number with the acetylethyne exposure. The apparent formation of darkened sites was previously observed in the adsorption of other small molecules, such as NH_3,[26] H_2O,[27] C_2H_2,[9] C_2H_4,[28] C_6H_6,[29] C_6H_5Cl,[30] and C_4H_4S[11] on Si(111)-7 × 7. In all these cases, the darkening of adatoms in STM images was attributed to the consumption of the adatom dangling bonds due to the surface−adsorbate bond formation. We found no bias dependence for the intensity at the reacted adatoms (darkened sites), suggesting that the adsorbed acetylethyne and reacted adatoms do not have orbitals close to the Fermi level E_F.

A statistical counting of darkened dangling bond sites can provide information on the spatial selectivity for acetylethyne chemisorption. Careful analysis of STM images (not shown) obtained after several different exposures of acetylethyne manifests the preferential adsorption on the center adatom sites of faulted halves. The results also show that the reactivity of center adatoms is about twice that of corner adatoms. At saturated chemisorption (Figure 5b), substantial adsorption also occurs on unfaulted halves. However, the preference of center adatoms over the corner adatom sites is still evident. The higher selectivity of acetylethyne binding to the faulted half and center adatom sites of a Si(111)-7 × 7 unit cell can be understood when considering the higher electrophilicity of the faulted subunits[31] and a smaller strain for molecules binding on the center adatom.[26] Furthermore, it was found that, with increased coverage, the maximum number of adatoms involved in acetylethyne chemisorption for every faulted or unfaulted half unit cell is three, equal to the number of the rest atoms. Thus, it is reasonable to deduce that every acetylethyne molecule binds with the neighboring adatom−rest atom pair.

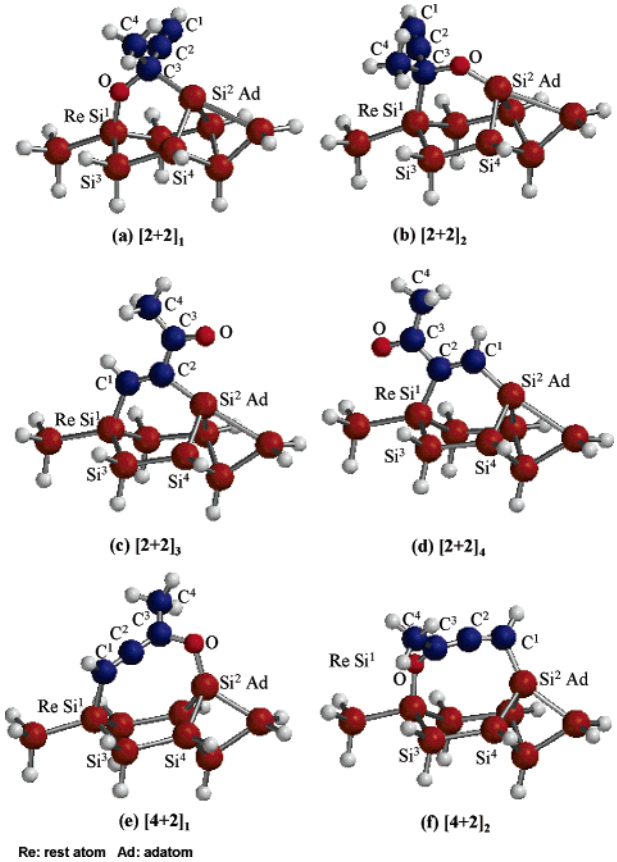

Figure 6. Optimized C_4H_4O/Si_9H_{12} clusters corresponding to the six possible attachment modes through [2 + 2]-like cycloadditions via a carbonyl or C≡C group and [4 + 2]-like addition reactions via the two terminal atoms of acetylethyne.

III.D. Density Functional Theory Calculations. In general, there are three possible ways for acetylethyne binding on Si(111)-7 × 7: (a) [2 + 2]-like cycloaddition through the C═O group; (b) [2 + 2]-like cycloaddition through the C≡C group; (c) [4 + 2]-like cycloaddition through the terminal C and O atoms of CH≡C−C(CH$_3$)═O. DFT theoretical calculations were carried out to obtain the optimized geometric structures and energies for these possible adsorption configurations.

In modeling, a Si cluster of $Si_{30}H_{28}$ was cut from the central part of MMFF94[32] optimized cluster, where the precision of atomic positions suffers the least from boundary effects. It contains an adatom and an adjacent rest atom from an unfaulted subunit, serving as a binding site for the attachment of one acetylethyne molecule. Capping H atoms at the cluster boundaries are kept frozen. Silicon atoms in the bottom double layers are placed at bulk lattice positions prior to the geometry optimization process, with each Si−Si bond length set to 2.3517 Å and all bond angles adjusted to 109.4712°. A smaller structure of Si_9H_{12} was obtained from further reduction of $Si_{30}H_{28}$. Similarly, all capping H atoms were frozen during geometry optimization. Clusters corresponding to the six possible binding models were constructed by acetylethyne adsorption onto the mother cluster (Si_9H_{12}). These Si clusters were previously used in the successful prediction of the adsorption energy of benzene on Si(111)-7 × 7,[33] and the most stable binding configurations of acetonitrile,[34] acrylonitrile,[13] and benzonitrile[35] on Si(111)-7 × 7.

Calculations were performed using the SPARTAN package.[36] The formation heats of chemisorbed configurations were calculated at the DFT theory level using perturbative Beck−Perdew functional (pBP86) in conjugation with a basis set of

TABLE 2: Adsorption Energies of Local Minima in the C_4H_4O/Si_9H_{12} Model System from pBP/DN

functional group	$C^3{=}O$	$C^3{=}O$	$C^1{\equiv}C^2$	$C^1{\equiv}C^2$	$C^1{\equiv}C^2{-}C^3{=}O$	$C^1{\equiv}C^2{-}C^3{=}O$
reaction model	$[2+2]_1$	$[2+2]_2$	$[2+2]_3$	$[2+2]_4$	$[4+2]_1$	$[4+2]_2$
adsorption energy[a]	25.5	26.4	56.0	54.6	76.3	82.6

[a] Adsorption energy: $\Delta E = [E(Si_9H_{12}) + E(C_4H_4O)] - E(C_4H_4O/Si_9H_{12})$. All energies are in kcal mol^{-1}.

TABLE 3: Fitted Results of XPS Spectra from Chemisorbed and Physisorbed Acetylethyne on Si(111)-7 × 7[a]

$HC^1{\equiv}C^2{-}C^3(C^4H_3){=}O$	physisorption	chemisorption	downshift	rehybridization
O	533.4	532.2	1.2	$sp^2{-}sp^3$
C^1	285.4	284.1	1.3	$sp{-}sp^2$
C^2	285.4	285.2	0.2	$sp{-}sp$
C^3	289.0	286.0	3.0	$sp^2{-}sp^2$
C^4	284.1	284.1	0	$sp^3{-}sp^3$

[a] All energies are in eV.

DN** (comparable 6-31G**).[36] Geometric optimizations were conducted under SPARTAN default criteria. Adsorption energy, synonymous to formation heat, is quoted here as the difference between the energy of the adsorbate/substrate complex and the total sum of the substrate and gaseous molecule. Figure 6 presents the six optimized geometries of the local minima for the acetylethyne/Si_9H_{12} model system. Their adsorption energies are given in Table 2. The calculation result reveals that the [4 + 2]-like cycloadditions are thermodynamically favored compared to the [2 + 2]-like cycloadditions. Cluster $[4+2]_2$ (Figure 6f) is seen to be most stable, where the O and C^1 atoms are linked to the adatom and rest atom to form a structure containing cumulative double bonds (C═C═C). This process is exothermic by 82.6 kcal mol^{-1}. In addition, the calculated vibrational frequencies (Table 1) of the most stable intermediate, cluster $[4+2]_2$ (Figure 6f), are consistent with our experimental vibrational spectrum.

IV. Discussion

Figure 6 presents six possible binding modes of acetylethyne on Si(111)-7 × 7. The [2 + 2]-like cycloaddition through the carbonyl group forms a surface intermediate of $C^1H{\equiv}C^2{-}C^3(Si)(C^4H_3){-}O(Si)$ (Figure 6a,b). In this reaction product, the C≡C group is retained. However, the disappearance of ≡CH (at 3240 cm^{-1}) and C≡C (at 2100 cm^{-1}) stretching modes in our HREELS results rules out this possiblility. The [2 + 2]-like reaction through the C≡C group to a neighboring adatom−rest atom pair gives a chemisorbed species of $(Si)C^1H{=}C^2(Si){-}C^3(C^4H_3){=}O$ (Figure 6c,d) with a $C^1{=}C^2{-}C^3{=}O$ conjugated structure. In these cycloadducts, both C^1 and C^2 atoms rehybridize from sp into sp^2, together with the retention of the carbonyl group. The disappearance of C═O (at 1684 cm^{-1}) stretching mode in the chemisorbed molecules also excludes these modes.

In fact, our results are consistent with the [4 + 2]-like cycloaddition reaction mechanism, forming a product containing a $-C^1H{=}C^2{=}C^3(C^4H_3){-}O$ skeleton (Figure 6e,f). In this structure, the disappearance of $C^3{=}O$ is expected, together with the conversion of $C^1{\equiv}C^2$ to $C^1{=}C^2$ upon cycloaddition. The characteristic C═C═C skeleton of the surface intermediate is further confirmed by the detection of its asymmetric stretching mode at 1921 cm^{-1}, together with its torsion (at 846 cm^{-1}) and bending (361 cm^{-1}) modes. Hence, the vibrational characteristics allow us to conclude that acetylethyne covalently bonds to the Si surface principally through breaking both $\pi_{C=O}$ and $\pi_{C\equiv C}$ bonds to react with the dangling bonds located on the adjacent adatom−rest atom pair via the [4 + 2]-like process.

The deconvoluted C 1s XPS data obtained from chemisorbed acetylethyne (Figure 4b) can be reasonably explained by the [4 + 2]-like cycloaddition. These constituent C 1s peaks can be attributed to the C^3(286.0 eV), C^2(285.2 eV), and C^1/C^4(284.1 eV) of the reaction adduct $(Si)C^1H{=}C^2{=}C^3(C^4H_3){-}O(Si)$. Table 3 lists the detailed assignment of C 1s and O 1s core levels for physisorbed and chemisorbed acetylethyne on Si(111)-7 × 7. This assignment is justified and consistent if comparison with previous studies is made. The C^1 atom with sp^2 hybridization in chemisorbed acetylethyne is chemically analogous to the C atoms of chemisorbed acetylene on Si(111)-7 × 7, giving similar binding energies (284.0 eV) for C 1s photoemission.[37] Since the C^4 of C^4H_3 is not involved in the surface reaction, it retains its C 1s value of 284.1 eV. The C^2 retains the sp hybridization in the chemisorbed state. Thus, its C 1s binding energy (285.2 eV) is not expected to shift significantly from the value (285.4 eV) of physisorbed molecules. The C^3 atom is related to C 1s peak at 286.0 eV. Although the C^3 atom retains the same sp^2 hydridization upon chemisorption, its C 1s BE downshifts by ∼3.0 eV referenced to the value of physisorbed acetylethyne. The rehybridization of the oxygen atom and its bonding to a Si atom with a much lower electronegativity (Pauling electronegativity = 1.90) reduce the electronic polarization in the $C^3{-}O$. Thus, compared to physisorbed acetylethyne, a much higher electron density is expected at the C^3 atom, leading to a lower C 1s BE of the C^3 atom.

The reactivity of acetylethyne on Si(111)-7 × 7 can also be reasonably explained considering the spatial arrangements of the acetylethyne molecule and the neighboring adatom−rest atom pair on the surface. The distance between the two terminal C and O atoms in $CH{\equiv}C{-}C(CH_3){=}O$ matches well with the separation of 4.5 Å between the adatom and its adjacent rest atom. However, great structural strains may exist in the $-(Si)C{-}O(Si)$ or $-(Si)C{=}CH(Si)$ formed through the [2 + 2]-like addition of C═O or C≡C groups, respectively, implying the instability of [2 + 2]-like cycloadducts.

For acetylethyne binding to a pair of adatom and rest atom through its C^1 and O atoms, there are two types of configurations, that is, O atom binding to the rest atom (Figure 6e) or to the adatom (Figure 6f). According to our calculation results, the binding state with O atom linking to an adatom is significantly more stable (by more than 6 kcal mol^{-1}) than the alternative configuration with O atom binding to a rest atom. On the other hand, the selective attachment of oxygen atom to the adatom over the rest atom is possibly attributable to a barrierless pathway passing through a dative-bonded precursor.[38] The oxygen atom has a couple of lone-pair electrons. Thus, it can possibly act as a donor to provide electrons to form a dative-bonded precursor with electron-deficient Si dangling bonds on adatoms, lowering the energy barrier of the surface reaction. This possibly explains the selectivity from the kinetic point of

view. Thus, the formation of cumulative double bonds (C═C═C) through the [4 + 2]-like cycloaddition of acetylethyne with Si dangling bonds on Si(111)-7 × 7 is thermodynamically and kinetically preferred.

V. Conclusions

The formation of (Si)C^1H═C^2═C^3(C^4H)−O(Si)-like surface intermediates in acetylethyne adsorption on Si(111)-7 × 7 is clearly demonstrated in our HREELS, XPS, STM, and DFT studies. The surface reaction occurs mainly through a [4 + 2]-like cycloaddition pathway between the adjacent adatom−rest atom pair and the two terminal atoms (O and C^1) of the molecule. The resulting cumulative double bonds C═C═C may be considered as a precursor for further dry organic syntheses and modification of silicon surfaces.

References and Notes

(1) Meyer zu Heringdorf, F.-J.; Reuter, M. C.; Tromp, R. M. *Nature* **2001**, *412*, 517−520.
(2) Yates, J. T., Jr. *Science* **1998**, *279*, 335−336.
(3) Lopinski, G. P.; Moffatt, D. J.; Wayner, D. D. M.; Wolkow, R. A. *Nature* **1998**, *392*, 909−911.
(4) Takayanagi, K.; Tanishiro, Y.; Takahashi, M.; Takahashi, S. *J. Vac. Sci. Technol.* **1985**, *3*, 1502−1506.
(5) Chadi, D. J.; Bauer, R. S.; Williams, R. H.; Hansson, G. V.; Bachrach, R. Z.; Mikkelsen, J. C., Jr.; Houzay, F.; Guichar, G. M.; Pinchaux, R.; Petroff, Y. *Phys. Rev. Lett.* **1980**, *44*, 799−802.
(6) Rochet, F.; Jolly, F.; Bournel, F.; Dufour, G.; Sirotti, F.; Cantin, J. L. *Phys. Rev. B* **1998**, *58*, 11029−11042.
(7) Carbone, M.; Zanoni, R.; Piancastelli, M. N.; Comtet, G.; Dujardin, G.; Hellner, L.; Mayne, A. *J. Electron. Spectrosc. Relat. Phenom.* **1995**, *76*, 271−276.
(8) Rochet, F.; Dufour, G.; Prieto, P.; Sirotti, F., Stedile, F. C. *Phys. Rev. B* **1998**, *57*, 6738−6748.
(9) Yoshinobu, J.; Fukushi, D.; Uda, M.; Nomura, E.; Aono, M. *Phys. Rev. B* **1992**, *46*, 9520−9524.
(10) Weiner, B.; Carmer, C. S.; Frenklach, M. *Phys. Rev. B* **1991**, *43*, 1678−1684.
(11) Cao, Y.; Yong, K. S.; Wang, Z. Q.; Chin, W. S.; Lai, Y. H.; Deng, J. F.; Xu, G. Q. *J. Am. Chem. Soc.* **2000**, *122*, 1812−1813.
(12) Cao, Y.; Wang, Z. H.; Deng, J. F.; Xu, G. Q. *Angew. Chem., Int. Ed.* **2000**, *39*, 2740−2743.
(13) Tao, F.; Chen, X. F.; Wang, Z. H.; Xu, G. Q. *J. Am. Chem. Soc.* **2002**, *124*, 7170−7180.
(14) Cao, Y.; Yong, K. S.; Wang, Z. H.; Deng, J. F.; Lai, Y. H.; Xu, G. Q. *J. Chem. Phys.* **2001**, *115*, 3287−3296.
(15) Moulder, J. F.; Stickle, W. F.; Sobol, P. E.; Bomben, K. D. *Handbook of X-ray Photoelectron Spectroscopy*; Physical Electronics Division, Perkin-Elmer Corporation: MN, 1991.
(16) Crowder, G. A. *Spectrochim. Acta, Part A* **1973**, *29*, 1885−1889.
(17) Chabal, Y. J.; Raghavachari, K. *Phys. Rev. Lett.* **1984**, *53*, 282−285.
(18) Daimay, L. V.; Norman, B. C.; William, G. F.; Feanette, G. G. *The Handbook of Infrared and Raman Characteristic Frequencies of Organic Molecules*; Academic Press: Boston, 1991.
(19) Wotiz, J. H.; Mancuso, D. E. *J. Org. Chem.* **1957**, *22*, 207−211.
(20) Wotiz, J. H.; Celmer, W. D. *J. Am. Chem. Soc.* **1952**, *74*, 1860−1861.
(21) Huang, J. Y.; Huang, H. G.; Lin, K. Y.; Liu, Q. P.; Sun, Y. M.; Xu, G. Q. *Surf. Sci.* **2004**, *549*, 255−264.
(22) Bu, Y.; Breslin, J.; Lin, M. C. *J. Phys. Chem. B* **1997**, *101*, 1872−1877.
(23) Lu, X.; Lin, M. C. *Int. Rev. Phys. Chem.* **2002**, *21*, 137−184.
(24) Tao, F.; Qiao, M. H.; Zhen, H. L.; Yang, L.; Dai, Y. J.; Huang, H. G.; Xu, G. Q. *Phys. Rev. B* **2003**, *67*, 115334-(1-7).
(25) Armstrong, J. L.; White, J. M.; Langell, M. *J. Vac. Sci. Technol., A* **1997**, *15*, 1146−1154.
(26) Avouris, Ph.; Wolkow, R. A. *Phys. Rev. B* **1989**, *39*, 5091−5100.
(27) Avouris, Ph.; Lyo, I. W. *Surf. Sci.* **1991**, *242*, 1−11.
(28) Yoshinobu, J.; Tsuda, H.; Onchi, M.; Nishijima, M. *Chem. Phys. Lett.* **1986**, *130*, 170−174.
(29) Wolkow, R. A.; Moffatt, D. J. *J. Chem. Phys.* **1995**, *103*, 10696−10700.
(30) Chen, X. H.; Kong, Q.; Polanyi, J. C.; Rogers, D.; So, S. *Surf. Sci.* **1995**, *340*, 224−230.
(31) Brommer, K. D.; Galvan, M.; Dal Pino, A., Jr.; Joannopoulos, J. D. *Surf. Sci.* **1994**, *314*, 57−70.
(32) Halgren, T. A. *J. Comput. Chem.* **1996**, *17*, 490−519.
(33) Wang, Z. H.; Cao, Y.; Xu, G. Q. *Chem. Phys. Lett.* **2001**, *338*, 7−13.
(34) Tao, F.; Chen, X. F.; Wang, Z. H.; Xu, G. Q. *J. Phys. Chem. B* **2002**, *106*, 3890−3895.
(35) Tao, F.; Wang, Z. H.; Chen, X. F.; Xu, G. Q. *Phys. Rev. B* **2002**, *65*, 115311(1-9).
(36) Hehre, W. J.; Yu, J.; Klunzinger, P. E.; Lou, L. *A Brief Guide to Molecular Mechanics and Quantum Chemical Calculation*; Wavefunction: Irvine, CA, 1998.
(37) Rochet, F.; Dufour, G.; Stedile, F. C.; Sirotti, F.; Prieto, P.; Crescenzi, M. De. *J. Vac. Sci. Technol., B* **1998**, *16*, 1692−1696.
(38) Barriocanal, J. A.; Doren, D. J. *J. Am. Chem. Soc.* **2001**, *123*, 7340−7346.